

Demonstration of 4π and 2π rotational symmetry in a spin-1 system (deuterons)

M. E. Stoll,* E. K. Wolff, and M. Mehring

Institut für Physik, Universität Dortmund, 46 Dortmund, Federal Republic of Germany

(Received 16 November 1977)

The sign reversal of the wave function under a 2π rotation ("spinor character") is demonstrated in a spin-1 system (deuterium) when only a two-level subsystem is irradiated. Under irradiation of all three levels of the system 2π symmetry is recovered, and a continuous variation from 4π to 2π symmetry is demonstrated by irradiation with two different, continuously adjustable asynchronous rf fields.

I. INTRODUCTION

It has been a well-established theoretical fact since the time of Pauli, that a particle with half-integral spin (fermion) exhibits a reversal of the sign of its wave function upon 2π rotation, and that the wave function changes back to its original state only after a full 4π rotation. Contrastingly, a particle with integral spin (boson) exhibits no such sign reversal of its wave function upon a 2π rotation. These fermion and boson phenomena are loosely termed as spinor and nonspinor character, respectively. The spinor behavior may be stated in a general way as

$$\exp(-i2\pi\vec{I}\cdot\vec{n})|\psi\rangle = -|\psi\rangle,$$

where \vec{n} is a unit vector in direction of axis of rotation, \vec{I} is a spin- $\frac{1}{2}$ operator and $|\psi\rangle$ a fermion wave function.

Although spinor character is implicit in many experiments, methods of explicitly observing this behavior were suggested by Bernstein¹ and by Aharonov and Susskind.² Neutron-beam interferometry experiments have shown spinor character for neutrons.^{3,4} Molecular-beam-resonance experiments⁵ and NMR interferometric experiments⁶ have also explicitly demonstrated spinor behavior for pseudo-two-level systems, and recent NMR interferometric experiments have attempted to exploit this behavior.^{7,8} However, all of these demonstrations have shown spinor behavior in systems comprised of fermions. In this paper we demonstrate spinor character in a boson system (deuteron) by utilizing NMR interferometry. This is done by arranging the experiment so that we first deal with only a pseudo-two-level system. Thus spinor character under rotation depends purely on whether the number of levels in our subsystem is even or odd, and not in any way upon whether or not the constituent particles comprising the entire level manifold are fermions or bosons. Furthermore we investigate and contrast in some detail the behavior of the full three-level relative to the two-level

subsystem. Finally, we show that by adjusting the relative amplitudes of our irradiation, we can go continuously from a two-level to a three-level system and thus continuously from 4π to 2π symmetry.

II. EXPERIMENTAL DETAILS

In order to show spinor character in a boson system, we chose a spin-1 nucleus, deuterium. Figure 1 shows the energy-level diagram of non-interacting deuterium nuclei. If there is only a large magnetic field, the three energy levels of the Zeeman Hamiltonian have equal spacing ω_0 . If there is an electric field gradient at the nucleus, then the levels will be further split to yield two inequivalent transition frequencies $\omega_0 + \omega_Q$ and $\omega_0 - \omega_Q$. It is important that we have such a difference between the two transition frequencies to enable us to selectively irradiate one transition and not the other, by using radiation weak compared to the splitting $2\omega_Q$. In this way we can hit only one transition (a two-level system), both transitions (a three-level system), or any continuous mixture in between.

The chemical system we selected was 98%-deuterated hexamethyl benzene (HMB). We performed the experiment in a superconducting magnet at a field of 4.2 T, where deuterium resonates at 27.6 MHz. We oriented a single crystal of the material to get the largest value of $2\nu_Q$ equal to about 32.5 kHz. At room temperature the benzene ring is rotating about its sixfold axis, and the methyl groups are "spinning." Thus there is a good deal of motion and therefore only an averaged quadrupole interaction is observed and all deuterium nuclei are magnetically equivalent. The motion also reduces T_1 to about 0.5 sec. The two NMR lines have a linewidth of about 1.2 kHz, owing primarily to deuterium-deuterium dipolar homogeneous broadening and secondarily to quadrupolar inhomogeneous broadening from crystal imperfections.

The spectrometer was a home-built unit, utiliz-

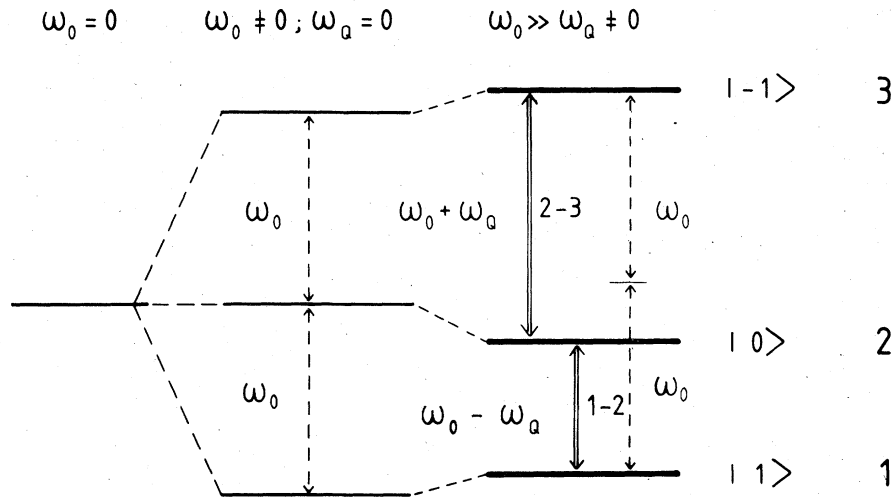


FIG. 1. Energy diagram of a spin-1 particle with quadrupole interaction ω_Q in a magnetic field $H_0 = \omega_0/\gamma$. The eigenstates of the three-level system are designated 1, 2, and 3. The two "allowed" transitions in first order 1-2 ($\omega_0 - \omega_Q$) and 2-3 ($\omega_0 + \omega_Q$) are indicated.

ing two independent frequency sources to irradiate the two frequencies. A discussion of phase relationships of such asynchronous sources to the observed magnetization will be presented in a forthcoming paper.⁹ Since we needed to use weak rf radiation compared to the splitting, we were able to do the experiment with values of the amplitude of the rf magnetic field in the rotating frame of about 5 G corresponding to only 1 W of power. Also since the splitting was small, we were easily able to irradiate both lines in a single resonance probe with a Q of about 50. A spherically cut crystal of about a 4-mm diameter was used for the sample.

III. SPINOR BEHAVIOR

In order to show spinor character, we employ the method of resonance interferometry.^{6,7} In this method we observe the overall phase of the quantum-mechanical wave function of a two-level subsystem by observing the relative phases of one of these levels with respect to a third reference level. This is done by monitoring an observable (in our case, a transverse dipolar magnetization) whose expectation value is proportional to the cosine of this relative phase difference. The pulsing scheme in Figure 2 illustrates how this was done in the lab. First of all we prepare a state of phase coherence between levels 1 and 2 by applying a pulsed rf field of duration t_p , which in effect rotates the two wave functions $|1\rangle$ and $|2\rangle$ by $\frac{1}{2}\pi$ about the x direction in the corresponding rotating frame, i.e., the operation of the rf field can be represented as $\exp(-i\beta_{12}I_x^{1-2})$, with $\beta_{12} = \frac{1}{2}\pi$ and where I_x^{1-2} is a fictitious spin- $\frac{1}{2}$ operator of the 1-2 transition.^{11(a),11(b)} This is followed by a pulsed rf field applied to the 2-3 transition, which

in effect rotates the wave function $|2\rangle$ and $|3\rangle$ by the angle β_{23} , i.e., these wave functions are transformed by $\exp(-i\beta_{23}I_x^{2-3})$, where I_x^{2-3} is a fictitious spin- $\frac{1}{2}$ operator of the 2-3 transition.^{11(a),11(b)} If β_{23} is chosen as 2π then the 2-3 two-level subsystem undergoes a change of sign, i.e., the overall phase of the subsystem changes by π . This causes the relative phase difference between 1 and 2 to change by π , thus causing the 1-2 magnetization to invert. These are the essential parts of the experiment. However, in order to make the effects we want to demonstrate more clearly visible, we have added some state-of-the-art NMR pulse technique as is described in the following.

A second rf pulse was applied to the 1-2 transition in order to create an echo of the 1-2 mag-

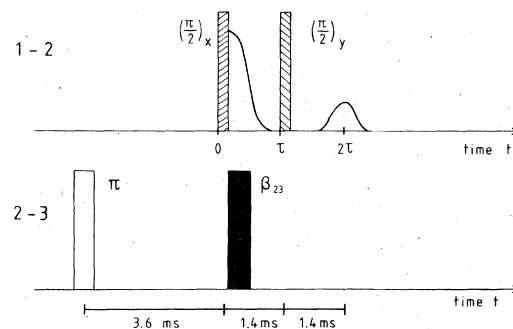


FIG. 2. Timing of the rf fields applied at the transitions 1-2 and 2-3. The prepulse (π pulse) at the 2-3 transition is applied only in order to avoid any unwanted magnetization transfer as explained in the text. The echo signal is phase sensitive and monitors the relative phase state of the 1-2 two-level subsystem as influenced by the rotation due to β_{23} at the 2-3 transition.

netization. This was not necessary for the experiment, but it was convenient, since during the β_{23} pulse, dipole-dipole interaction caused some loss of 1-2 magnetization. This was similar to the echo method of Stoll *et al.*^{6,7} except that in those experiments there was inhomogeneous broadening and a π pulse was used to refocus magnetization, but in our case there was homogeneous broadening so we used at time τ a $\frac{1}{2}\pi$ pulse shifted in phase by $\frac{1}{2}\pi$ to create a solid dipolar echo¹⁰ at time 2τ .

In addition, a π prepulse was used on the 2-3 transition a "long time" before the actual experiment. This also was not necessary, but rather convenient. Without it we found for values of $\beta_{23} \neq 0, 2\pi, \dots$ that magnetization on the 1-2 channel immediately following the $\frac{1}{2}\pi$ echo pulse interfered with observation of the echo signal. This is understandable in terms of the populations of the various energy levels.

Without the prepulse, the first $\frac{1}{2}\pi$ pulse on the 1-2 transition creates transverse magnetization and equalizes the population of levels 1 and 2. The β_{23} pulse then (for $\beta_{23} \neq 0, 2\pi, \dots$) changes the population of levels 2 and 3, thus making levels 1 and 2 no longer having the same population. Thus the $\frac{1}{2}\pi$ echo pulse on 1-2 creates new magnetization from this population difference, and it interferes with the echo. This problem becomes very severe when $\beta_{23} = \pi$ and the population of 2 and 3 are inverted. This difficulty was alleviated by making a π prepulse on the 2-3 transition. Since $\omega_0 \gg \omega_Q$ the thermal equilibrium population difference between levels 1 and 2 is very close to that of 2 and 3. Thus we can consider the population of the levels at equilibrium to be, in the high-temperature approximation,

$$N_1 = \frac{1}{3}N + \Delta, \quad N_2 = \frac{1}{3}N, \quad N_3 = \frac{1}{3}N - \Delta, \quad (1)$$

where N is the total number of spins and $\Delta = N\hbar\omega_Q/3kT$. After the π prepulse they become

$$N_1' = \frac{1}{3}N + \Delta, \quad N_2' = \frac{1}{3}N - \Delta, \quad N_3' = \frac{1}{3}N. \quad (2)$$

The first $\frac{1}{2}\pi$ pulse on the 1-2 transition now makes

$$N_1'' = N_2'' = N_3'' = \frac{1}{3}N. \quad (3)$$

So now the β_{23} pulse cannot cause any problems, because the populations of 2 and 3 are the same, and the subsequent 1-2 echo pulse still creates an echo but does not create new 1-2 magnetization immediately. One very important additional benefit of the prepulse is that it creates a factor-of-2 enhancement of the 1-2 signal by doubling the population difference of 1 and 2 before the first $\frac{1}{2}\pi$ pulse on the 1-2 channel (pseudo-Overhauser enhancement). Since the population inversion created by the prepulse lasted for the time of spin-lattice relaxation T_1 , we spaced it early enough in time

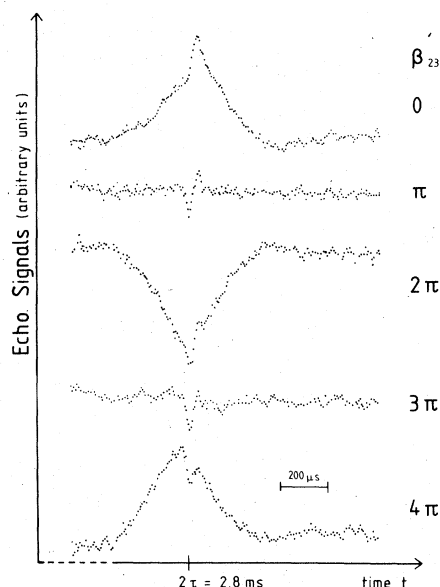


FIG. 3. Echo amplitude at the 1-2 transition as influenced by the rotation β_{23} at the 2-3 transition in the case of deuterated hexamethyl benzene. The sign reversal for a 2π rotation ($\beta_{23} = 2\pi$) is clearly visible and the 4π symmetry is evident. The "dispersionlike" signal on top of the ordinary echo is due to crystal imperfections. This signal does not follow a pure rotation by β_{23} and is therefore ignored here.

that any 2-3 transverse magnetization we might have made by virtue of the prepulse not being a perfect π pulse would have disappeared and could not have been inadvertently refocused by the β_{23} pulse during the time scale of our experiment.

Examples of the 1-2 echoes, created by the pulse sequence of Fig. 2, are shown in Fig. 3. These are the actual echo signals in the time domain, signal averaged about 100 times. Echo signals are shown for values of $\beta_{23} = 0, \pi, 2\pi, 3\pi, 4\pi$.

The initial free-induction decays (FID) are about a factor of 30 larger than the echoes. This is because we chose a long time $\tau = 1.4$ msec compared to the decay time of the magnetization (about 300 μ sec) in order to see a well-resolved echo, and because there was some inhomogeneous broadening not totally refocused by the solid echo pulse.

One notes immediately from Fig. 3 that the 1-2 echo inverts after a rotation of $\beta_{23} = 2\pi$ and is non-inverted again after a 4π rotation. This clearly shows the spinor character of the 2-3 two-level subsystem, in spite of the fact that these levels are part of a boson, three-level manifold. For a $\beta_{23} = 2\pi$ rotation, overall phase of levels 2 and 3 changes by π (since $e^{i\pi} = -1$, the sign of the wave function for 2, 3 changes) and thus the relative phase of 1 and 2, as defined by the initial $\frac{1}{2}\pi$ pulse

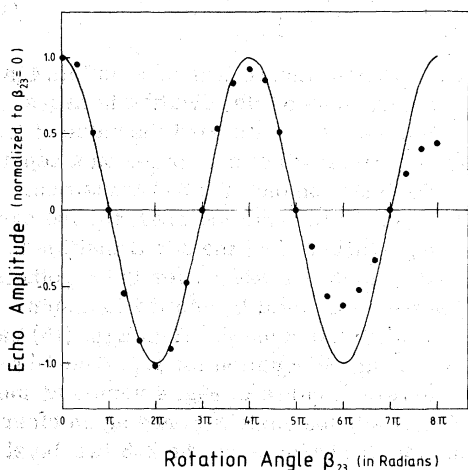


FIG. 4. Normalized echo amplitude at the 1-2 transition vs the rotation angle β_{23} at the 2-3 transition, obtained from data as shown in Fig. 3. The experimental data represent a damped cosine function, whereas the solid line represents the theoretical $\cos(\frac{1}{2}\beta_{23})$ behavior. Note again the 4π rotational symmetry.

changes by π , causing the magnetization and the subsequent echo to invert. For $\beta_{23} = 4\pi$, the overall phase of levels 2 and 3 changes by 2π (since $e^{i2\pi} = +1$, the sign of the wave function for 2, 3 does not change) and the relative phase of 1 and 2 changes by 2π , causing the magnetization and subsequent echo to be upright. Of course the same behavior is expected to be observed if a rf field $H_1 = \omega_1/\gamma$ is applied at the double quantum transition 1-3 with $\beta_{13} = (\omega_1^2/\omega_Q)t$ being the rotation angle.¹¹ Details of this will be presented elsewhere.⁹

We have measured the amplitude of the 1-2 echo for various values of β_{23} rotation angle through 8π and plotted them in Fig. 4. One again notes the 4π symmetry, characteristic of a spinor, which is how the 2-3 two-level subsystem behaves. The experimental data are indicated by large circles and the solid line is the theoretical prediction. The theory for this case of irradiating only β_{23} is quite simple and can be done easily. The nonspinor behavior as discussed later in the paper requires us to irradiate the 1-2 transition also, where $\beta_{12} = \beta_{23}$. Section V will discuss cases where $0 \leq \beta_{12} \leq \beta_{23}$. These will require a more elaborate treatment, so in Sec. IV we do a rigorous, general theory, which will apply for all cases. We will then return to the question of the theoretical curve of Fig. 4.

IV. THEORY

We now want a general formula for the density matrix of our three-level spin system after pulses

β_{12} and β_{23} are simultaneously applied to both transitions. We first consider our thermal equilibrium density matrix (high-temperature approximation) in the representation of the eigenstates of the Zeeman Hamiltonian,

$$\rho_{\text{eq}} = \begin{bmatrix} \frac{1}{3}N + \Delta & 0 & 0 \\ 0 & \frac{1}{3}N & 0 \\ 0 & 0 & \frac{1}{3}N - \Delta \end{bmatrix} \quad (4)$$

After the π prepulse on 2-3 and the initial $\frac{1}{2}\pi$ pulse on 1-2, we have

$$\rho(0) = \begin{bmatrix} \frac{1}{3}N & i\Delta & 0 \\ -i\Delta & \frac{1}{3}N & 0 \\ 0 & 0 & \frac{1}{3}N \end{bmatrix}, \quad (5)$$

assuming the initial $\frac{1}{2}\pi$ pulse on 1-2 is defined as having π phase.

Equation (5) can be rewritten slightly to yield

$$\rho(0) = \frac{1}{2}N\underline{1} + \begin{bmatrix} 0 & i\Delta & 0 \\ -i\Delta & 0 & 0 \\ 0 & 0 & 0 \end{bmatrix} \quad (6)$$

We will neglect the first term on the right-hand side of Eq. (6), because it remains invariant under any unitary transformation and hence remains an uninteresting constant in time.

Next we need to calculate the time development of this $\rho(0)$ under irradiation for a time t at both the 1-2 and 2-3 transitions. The Hamiltonian for the system during this time is

$$\mathcal{H} = -\omega_0 I_x + \frac{1}{3}\omega_Q(3I_x^2 - I^2) + 2\omega_{1a} \cos[(\omega_0 + \omega_Q)t + \frac{1}{2}\pi] I_x + 2\omega_{1b} \cos[(\omega_0 - \omega_Q)t + \frac{1}{2}\pi] I_x, \quad (7)$$

where we have Zeeman and quadrupolar interactions as well as rf applied at 1-2 frequency $(\omega_0 + \omega_Q)$ with a magnitude $2\omega_{1a}$ and rf applied at the 2-3 frequency with a magnitude $2\omega_{1b}$. Note that we have placed a phase shift of $\frac{1}{2}\pi$ in the 1-2 radiation. This will place it effectively along the y axis in the interaction frame, where it will be parallel to the 1-2 magnetization. This was done for a similar reason as the prepulse, i.e., to avoid magnetization formed immediately after the echo pulse from interfering with observation of the echo. (Interesting effects occur if one changes the phase of the 1-2 rf with respect to the existing 1-2 magnetization, and these will also be discussed in the previously mentioned upcoming paper,⁹ because they are not really pertinent to the questions at hand.)

We now choose to go to the interaction frame of the Hamiltonian

$$\mathcal{H}_0 = -\omega_0 I_x + \frac{1}{3}\omega_Q(3I_x^2 - I^2). \quad (8)$$

This is essentially the same transformation as that of Hartmann^{12(a)} and Chandra and Yen^{12(b)} and we will discuss the motivation for this transformation in our later paper.⁹ In this frame the remaining Hamiltonian $\tilde{\mathcal{H}}_1$ becomes

$$\tilde{\mathcal{H}}_{1 \text{ sec}} = \begin{bmatrix} 0 & -i\omega_{1a}/\sqrt{2} & 0 \\ i\omega_{1a}/\sqrt{2} & 0 & -i\omega_{1b}/\sqrt{2} \\ 0 & i\omega_{1b}/\sqrt{2} & 0 \end{bmatrix}, \quad (9)$$

where the tilde indicates we are in the interaction frame, and the subscript "sec" means that we have kept only the secular parts of the Hamiltonian, ignoring terms that oscillate rapidly, similar to the rotating-wave approximation.¹² Then by taking the time evolution of the density matrix as

$$\rho(t) = U(t)\rho(0)U^\dagger(t), \quad U(t) = e^{-i\tilde{\mathcal{H}}_{1 \text{ sec}}t}, \quad (10)$$

we have the following spin density matrix elements at time t .

$$\begin{aligned} \rho_{12}(t) &= i\Delta(R^2 + \cos\omega_1^*t)/(1+R^2), \\ \rho_{23}(t) &= i\Delta R(1 - \cos\omega_1^*t)/(1+R^2), \end{aligned} \quad (11)$$

where the parameters R and ω_1^* are defined as

$$R = \omega_{1a}/\omega_{1b}, \quad \omega_1^* = [\frac{1}{2}(1+R^2)]^{1/2}\omega_{1b}. \quad (12)$$

The other elements of $\rho(t)$ are not listed in Eq. (11) because they are not relevant to us now, since we will only be observing the transverse components of magnetization at frequencies 1-2 and 2-3. We use the following equations relating the density matrix to the expectation values of I_x and I_y at the two frequencies

$$\begin{aligned} \langle I_x \rangle_{12} &= c(\rho_{12} + \rho_{21}), & \langle I_y \rangle_{12} &= ic(\rho_{12} - \rho_{21}); \\ \langle I_x \rangle_{23} &= c(\rho_{23} + \rho_{32}), & \langle I_y \rangle_{23} &= ic(\rho_{23} - \rho_{32}), \end{aligned} \quad (13)$$

where c is a constant. We then have theoretical expressions for the transverse magnetization at time t as compared to the case for $t=0$,

$$\begin{aligned} \langle M_y(t) \rangle_{12} / \langle M_y(0) \rangle_{12} &= (R^2 + \cos\omega_1^*t)/(1+R^2), \\ \langle M_y(t) \rangle_{23} / \langle M_y(0) \rangle_{12} &= R(1 - \cos\omega_1^*t)/(1+R^2), \\ \langle M_x(t) \rangle_{12} &= \langle M_x(t) \rangle_{23} = 0. \end{aligned} \quad (14)$$

One particular limiting case for Eq. (14) is the case of Sec. III where we irradiated only the 2-3 transition. This corresponds to the case where $R=0$, which yields

$$\begin{aligned} \langle M_y(t) \rangle_{12} / \langle M_y(0) \rangle_{12} &= \cos\frac{1}{2}\beta_{23} \\ \langle M_y(t) \rangle_{23} &= 0, \quad \beta_{23} = \sqrt{2}\omega_{1b}t. \end{aligned} \quad (15)$$

So we see now that the theoretical curve in Fig. 4 is just $\cos\frac{1}{2}\beta_{23}$. A word of clarification is necessary at this point. We calibrated the value of β_{23} by measuring the length of a 2π pulse on a separate FID experiment on only the 2-3 transition. Due to the value of the spin matrix I_x for the case of $I=1$, the perturbation at the 2-3 transition is increased by a factor of $\sqrt{2}\omega_{1b}$ over the hypothetical case of the same field H_1 applied to a spin $I=\frac{1}{2}$ particle with the same γ . Thus Eqs. (15) have an "extra" $\sqrt{2}$ in the equation for β_{23} . The fact that the theoretical curve in Fig. 4 varies as the cosine of *one-half* the angle β_{23} once again clearly shows the spinor character of the 2-3 two-level subsystem.

The experimental points seem to follow more of a damped cosine function. This damping can be explained by an rf inhomogeneity of about 15%. However, it may also be due to relaxation effects similar to those reported in the spinor experiments in a liquid.⁷ Other extraneous effects can come about by having a small probability of not being able to irradiate only one transition,⁷ but in our experiment where values of $\nu_{1 \text{ eff}} = \sqrt{2}\omega_{1b}/2\pi$ were about 5 kHz, the important ratio of $\frac{1}{2}\sqrt{2}\omega_{1b}/2\omega_Q$ had a value of about 0.08, which was small enough for us to ignore such effects here.

V. BEHAVIOR OF A THREE-LEVEL SYSTEM UNDER ROTATION

In this section we want to study the properties of the entire three-level system while irradiating both transitions, and how these properties are different from the case of the two-level subsystem treated earlier.

In Figure 5 we show a plot of experimental echo amplitudes on both the 1-2 and 2-3 transitions as well as the corresponding theoretical curves. Note that here the curves have the 2π symmetry of the non-spinor. The experiment measuring the 1-2 echo (solid circles in Fig. 5) was done with the same pulse sequence of Fig. 2, except that now a pulse was also applied to the 1-2 transition simultaneously to the β_{23} pulse shown on the figure, and the rotation angle of β_{12} was chosen to be the same as β_{23} . During the β_{12} pulse the normal dipolar dephasing could not take place as usual, hence the echo would have formed earlier in time. So to counteract this, we set the echo delay time to be fixed with respect to the end of the β_{12} and β_{23} pulses. Thus all echoes had the same amount of dipolar evolution. The 2-3 echo data (open circles in Fig. 5) were taken as in Fig.

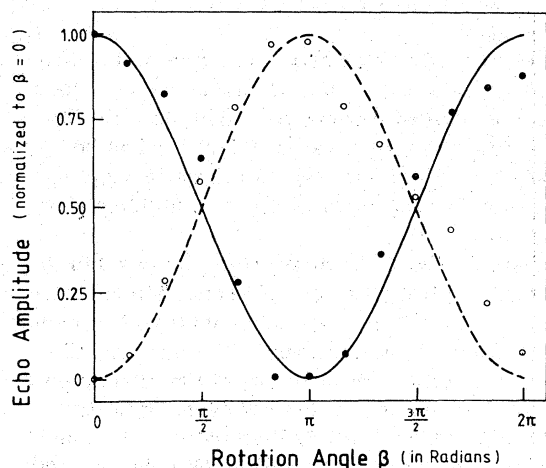


FIG. 5. Echo amplitudes of the 1-2 (●) and 2-3 (○) transitions, respectively, when rf fields are applied at both transitions simultaneously with the condition $\beta = \beta_{12}/\sqrt{2} = \beta_{23}/\sqrt{2}$. Here the relative phase between the $\frac{1}{2}\pi$ pulse and the β_{12} pulse is $\frac{1}{2}\pi$ corresponding to the spin-locking condition. Magnetization transfer with 2π symmetry is clearly demonstrated.

2 except with again the addition of the β_{12} pulse. One other difference is that the solid echo pulse was moved from the 1-2 to the 2-3 channel, thus enabling us to see a 2-3 solid dipolar echo instead.

Using the same phrasing we used earlier in the paper, the initial $\frac{1}{2}\pi$ pulse on 1-2 caused a coherent mixture of states $|1\rangle$ and $|2\rangle$. Then by irradiating this entire three-level system (with equal amplitudes at each frequency) and performing a 2π rotation we now change the overall phases corresponding to all three levels. This is fundamentally different than what we did in Sec. IV. Earlier we changed the phase corresponding to only levels 2 and 3. This left the phase of level 1 as a reference. However, in this case we now change the phase of level 1 also.

Thus we really are not doing the interferometry properly anymore, since if the overall phases of all levels change, then the relative phase of levels 1 and 2 does not change. Thus by irradiating both transitions we no longer can tell if our three-level system is behaving as a spinor or nonspinor since either case would yield the same 2π symmetry. Thus we call this "apparent" spinor behavior since it has 2π symmetry, but we can no longer say whether the system has real nonspinor behavior. In order to do this we would need a fourth level (which is not available) to use as a reference.

In addition this experiment is interesting from other points of view. The theoretical curves for

this experiment can be generated from Eq. (14) by taking the special case of $R = 1$ ($\omega_{1a} = \omega_{1b}$). This yields

$$\begin{aligned} \langle M_y(t) \rangle_{12} / \langle M_y(0) \rangle_{12} &= \frac{1}{2}(1 + \cos\beta), \\ \langle M_y(t) \rangle_{23} / \langle M_y(0) \rangle_{12} &= \frac{1}{2}(1 - \cos\beta), \end{aligned} \quad (16)$$

$$\beta = \omega_{1y}t.$$

Note that, however, the 2π periodicity is in fact only for β defined without the "extra" $\sqrt{2}$ in Sec. IV. This important theoretical point is clearly illustrated by the experimental data. Figure 5 shows the theoretical curves of Eq. (16) for 1-2 magnetization (solid line) and the 2-3 magnetization (dashed line) as well as the experimental data.

Another major difference between the $\beta_{12} = \beta_{23}$ case and the earlier $\beta_{12} = 0$ case is the magnetization is actually transferred from the 1-2 to the 2-3 frequency. This was not possible in the previous cases where $\beta_{12} = 0$. However, if we had not selectively created initial magnetization only on the 1-2 transition, this would not be observable. For instance, suppose $\omega_Q = 0$. In this case we would have identical initial magnetization on both frequencies. Then at each frequency we would see any initial magnetization remaining as well as any magnetization transferred from the other frequency. Thus both of these would superimpose at each frequency. Theoretically this just means adding the expressions of Eq. (16) to get $\langle M_y(t) \rangle_{12 \text{ or } 23} = \langle M_y(0) \rangle_{12 \text{ or } 23}$. Thus there would be no observable transfer. This would be perceived as a "spin-locking" pulse. So these Eqs.

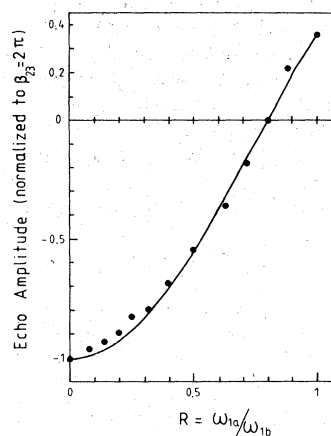


FIG. 6. Echo amplitude of the 1-2 transition with two different rf fields ω_{1a} (1-2) and ω_{1b} (2-3) applied at the same time under spin-locking conditions. The ratios $R = \omega_{1a}/\omega_{1b}$ was varied between $0 \leq R \leq 1$, whereas $\beta_{23} = 2\pi$ was fixed. Continuous variation from 4π to 2π symmetry is observed (see text).

(16) give us an insight into the way spin-locking works in a spin-1 system.

The final experiment we have done is shown in Fig. 6. Here we examine the behavior of the spin system at a fixed time for different values of the ratio R . We picked the case where when $R=0$, the 1-2 echo has been completely inverted. This means that the value of $\sqrt{2}\omega_{1b}t$ is chosen to be 2π . In this limit Eqs. (14) become

$$\langle M_y(t) \rangle_{12} / \langle M_y(0) \rangle_{12} = \{R^2 + \cos[(1+R^2)^{1/2}\pi]\} / (1+R^2), \quad (17)$$

$$\langle M_y(t) \rangle_{23} / \langle M_y(0) \rangle_{12} = R\{1 - \cos(1+R^2)^{1/2}\pi\} / (1+R^2).$$

This first theoretical equation is plotted in Fig. 6 along with experimental echo amplitudes of the 1-2 channel. We performed this experiment with the same pulse sequence as in Fig. 2, except that we have now applied a β_{12} pulse simultaneously to the β_{23} pulse. Although these pulses had the same time duration, the rotation angle β_{12} and β_{23} were not necessarily equal. This was arranged by leaving ω_{1b} fixed, while varying ω_{1a} from $\omega_{1a}=0$ to $\omega_{1a}=\omega_{1b}$ ($0 \leq R \leq 1$). We can see that the values range from -1 at $R=0$ to 0.37 at $R=1$. This change of sign is indicative of the continuous

change from 4π symmetry to 2π symmetry, and so we can follow just how the evidence of spinor character vanishes smoothly. The only reason that we do not have a value of 1 at $R=1$ is because of the $\sqrt{2}$ factor which means that for the case of $R=1$, the rotation angle is no longer 2π but rather $2\pi/\sqrt{2}$.

Finally it should be noted, that the problem of polarization transfer and coherent phenomena in three-level systems have been dealt with recently in a number of publications.^{13,14} However, the rotational symmetry of the wave function as emphasized in this paper has not been explicitly stated in a three-level system before. Further information on phase as well as on coherent and incoherent irradiation will be presented in a forthcoming paper.⁹

ACKNOWLEDGMENTS

Interesting discussions with Professor R. W. Vaughan and Professor A. Pines are gratefully acknowledged. The single crystal of deuterated HMB was grown by H. Zimmermann and kindly supplied to us by Professor Pines. The Deutsche Forschungsgemeinschaft has given a financial support.

*Present address: Sandia Laboratories 8342, Livermore, Calif. 94550.

¹H. J. Bernstein, Phys. Rev. Lett. **18**, 1102 (1967).

²Y. Aharonov and L. Susskind, Phys. Rev. **158**, 1237 (1967).

³H. Rauch, A. Zeilinger, G. Badurek, A. Wilfing, W. Bauspiess, and U. Bonse, Phys. Lett. **54A**, 425 (1975); G. Badurek, H. Rauch, A. Zeilinger, W. Bauspiess, and U. Bonse, Phys. Rev. D **14**, 1177 (1976).

⁴S. A. Werner, R. Colella, A. W. Overhauser, and C. F. Eagan, Phys. Rev. Lett. **35**, 1053 (1975).

⁵E. Klempt, Phys. Rev. D **13**, 3125 (1975).

⁶M. E. Stoll, A. J. Vega, and R. W. Vaughan, Phys. Rev. A **16**, 1521 (1977).

⁷M. E. Stoll, A. J. Vega, and R. W. Vaughan, J. Chem.

Phys. **67**, 2029 (1977).

⁸M. Polak and R. W. Vaughan (unpublished).

⁹M. E. Stoll, E. K. Wolff, and M. Mehring (unpublished).

¹⁰J. G. Powles and J. H. Strange, Proc. Phys. Soc. Lond. **82**, 4286 (1967).

¹¹(a) S. Vega and A. Pines, J. Chem. Phys. **66**, 5624 (1977); (b) A. Wokaun and R. R. Ernst, *ibid.* **67**, 1752 (1977); (c) A. Pines (private communication).

¹²(a) S. R. Hartmann, IEEE J. Quantum Electron. **4**, 802 (1968); (b) S. Chandra and W. M. Yen, Phys. Lett. **57A**, 217 (1976).

¹³H. Hatanaka, T. Terao, and T. Hashi, J. Phys. Soc. Jpn. **39**, 835 (1975).

¹⁴R. G. Brewer and E. L. Hahn, Phys. Rev. A **11**, 1641 (1975).